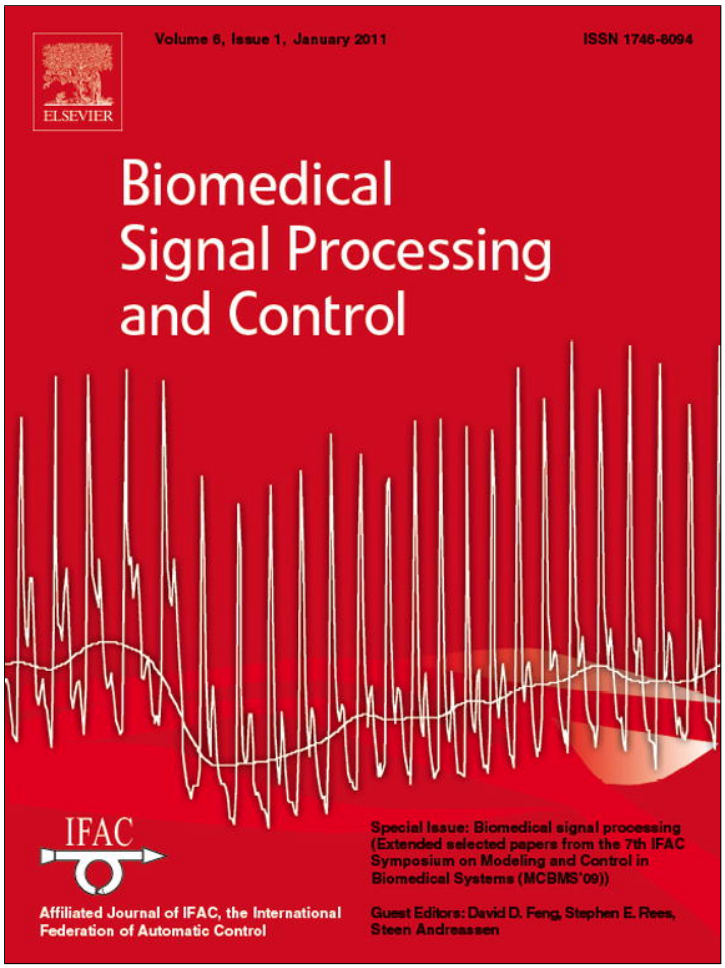

Biomedical Signal Processing and Control 6 (2011) 3–12

Contents lists available at ScienceDirect

Biomedical Signal Processing and Control

journal homepage: www.elsevier.com/locate/bspc

Intensity inhomogeneity compensation and segmentation of MR brain images using hybrid *c*-means clustering models

László Szilágyi[a,b,*], Sándor M. Szilágyi[a,1], Balázs Benyó[b,2], Zoltán Benyó[b,2]

[a] Sapientia University of Transylvania, Faculty of Technical and Human Sciences, Şoseaua Sighişoarei 1/C, 547367 Corunca, Romania
[b] Budapest University of Technology and Economics, Department of Control Engineering and Information Technology, Magyar tudósok krt. 2, H-1117 Budapest, Hungary

ARTICLE INFO

Article history:
Received 18 December 2009
Received in revised form 14 June 2010
Accepted 3 August 2010

Keywords:
Image segmentation
Intensity inhomogeneity
Magnetic resonance imaging
Fuzzy c-means clustering
Hybrid *c*-means clustering
Context dependent filter
Morphological operations

ABSTRACT

Medical image segmentation and registration problems based on magnetic resonance imaging are frequently disturbed by the intensity inhomogeneity or intensity non-uniformity (INU) of the observed images. Most compensation techniques have serious difficulties at high amplitudes of INU. This study proposes a multiple stage hybrid *c*-means clustering approach to the estimation and compensation of INU, by modeling it as a slowly varying additive or multiplicative noise. The slowly varying behavior of the estimated inhomogeneity field is assured by a context sensitive smoothing filter based on a morphological criterion. The qualitative and quantitative evaluation using 2-D synthetic phantoms and real T1-weighted MR images place the proposed methodology among the most accurate segmentation techniques in the presence of high-magnitude inhomogeneity.

1. Introduction

The segmentation of an image represents the separation of its pixels into non-overlapping, consistent regions, which appear homogenous with respect to some criteria concerning color and/or texture. MR brain image segmentation generally aims at separating white matter (WM) from gray matter (GM) and cerebrospinal fluid (CSF), which are usually distinguished by their intensity. The segmentation of MR images can support the qualitative and quantitative identification of various anatomical structures, thus providing important services to intelligent automated diagnosis systems.

Among the currently available medical imaging techniques, magnetic resonance imaging (MRI) has a relatively high resolution and good contrast, but it also suffers from three considerable obstacles: high-frequency noise (mixture of Gaussian and impulse noises), partial volume effect (pixels containing at least two types of tissues), and intensity inhomogeneity [1]. This latter one, also known as intensity non-uniformity (or INU artefact), manifests as a spatially slowly varying function that makes pixels belonging to the same tissue be observed having different intensities. In order to provide a correct segmentation of INU-contaminated MR images, this artefact needs to be modeled and compensated.

Inhomogeneities are generally categorized by their origin. Those related to the imaging device have efficient compensation and calibration methods like the usage of a uniform phantom to produce prior information [2]. On the other hand, INU artefacts related to the shape, position, structure and orientation of the patient [3], are much more difficult to handle [4].

Reported INU compensation methods use several different approaches. Early compensation methods like homomorphic filtering [5,6] were built upon the theoretical assumption that the frequency spectra of the image structures and of the INU artefact are not overlapping each other. Surface fitting methods engage a surface model (e.g. polynomial or B-spline) to approximate the inhomogeneity according to certain image features, which can be intensity based [7] or gradient based [8,9]. Segmentation based methods usually embed the INU compensation into an image segmentation process. These approaches implement maximum likelihood estimation [10,11], Markov random fields [12,13], fuzzy *c*-means clustering [1,14,15], or nonparametric estimation [16]. Further, histogram based INU compensation procedures involve high-frequency maximization [17], information maximization [18–20], or histogram matching [21,22].

* Corresponding author at: Sapientia University of Transylvania, Faculty of Technical and Human Sciences, Şoseaua Sighişoarei 1/C, 547367 Corunca, Romania. Tel.: +40 265 208170; fax: +40 265 206211.
E-mail addresses: lalo@ms.sapientia.ro (L. Szilágyi), szs@ms.sapientia.ro (S.M. Szilágyi), bbenyo@iit.bme.hu (B. Benyó), benyo@iit.bme.hu (Z. Benyó).
[1] Tel.: +40 265 208170; fax: +40 265 206211.
[2] Tel.: +36 1 463 1410.

1746-8094/$ – see front matter © 2010 Elsevier Ltd. All rights reserved.
doi:10.1016/j.bspc.2010.08.004

One of the most widely used INU compensation methods is the adaptation of the fuzzy *c*-means (FCM) clustering algorithm to iteratively approximate the INU as a smoothly varying bias or gain field. In this order, Pham and Prince introduced a modified objective function producing bias field estimation and containing extra terms that force this artefact vary smoothly [15]. They also provided a multigrid technique to speed up the computationally heavy algorithm, but even this way, their algorithm performs slowly. The same objective function was reached from a Bayesian approach in [23]. Liew and Hong created a log bias field estimation technique that models the INU with smoothing B-spline surfaces [24]. Ahmed et al. [25] established a regularization operator that allowed the labeling of a voxel to be influenced by its immediate neighbors. This approach reduced some of the complexity of its ancestors, but the zero gradient condition that was used for bias field estimation leads to several misclassifications. Siyal and Yu [1] provided a mean spread filtering method to smoothen the estimated bias field in every cycle of the FCM algorithm, thus reducing the amount of necessary computations, but the result of the segmentation is not deterministic due to the nature of the smoothing filter.

The theory of *c*-means clustering had a long evolution and it is still improving. Initially, there was the hard *c*-means algorithm (HCM) [26], which used the conventional bivalent logic to partition the input data, meaning that in any iteration, one item is assigned to exactly one class with 100% probability. HCM converges quickly, but often crashes and even if it doesn't, it gives a lot of misclassifications, due to its sensitivity to noise. A major improvement of the partition quality was produced by the fuzzy *c*-means clustering [27], but it hardly changed anything in the sensitivity to outliers. An efficient elimination of this latter problem was provided by the possibilistic *c*-means algorithm (PCM) [28]. This approach dropped the probabilistic constraint of the partition matrix: the degree to which an item belongs to a class does not anymore represent a probability. Instead of that, the possibilistic partition stores the typicality or compatibility of elements with different classes. Although the sensitivity to noises got an instant and efficient solution, some new problems emerged. Pure possibilistic *c*-means clustering, because of the excessive independency of its cluster prototypes, often comes up with coincident clusters [29]. This problem received several solutions afterwards, the most recent and most robust one being the fuzzy – possibilistic *c*-means hybrid given in [30]. On the other hand, the suppressed fuzzy *c*-means algorithm (s-FCM) [31], and its improved, optimal version (Os-FCM) [32] showed us some beneficial effects of mixing the fuzzy *c*-means clustering model with the hard one, at least from the point of view of execution speed.

All these clustering techniques suffer from sensitivity to high-amplitude INU artefacts: when the intensities of different tissue types overlap, segmentation accuracy falls, as the clustering algorithm is unable to correctly compensate the INU. In order to handle this problem, in this paper we propose a multi-stage *c*-means clustering based technique for bias- or gain field estimation of the inhomogeneity. Furthermore, we present two context sensitive filtering techniques to improve the segmentation accuracy. The prefiltering algorithm serves the elimination of high-frequency noises before segmentation, while the morphological criterion based smoothing filter is intended to guarantee the slow variation of the estimated INU artefact. The proposed methods are tested using real MR images and artificial phantoms.

The rest of the paper is organized as follows. Section 2 describes the background works based on fuzzy *c*-means clustering. Section 3 presents the details on the proposed filtering techniques and the multi-stage hybrid *c*-means clustering based bias- and gain field estimation approaches. Section 4 provides a qualitative and quantitative analysis and short discussion of segmentation results. In Section 5 the conclusions are formulated.

2. Background works

2.1. The evolution of c-means clustering models

After three decades of fruitful history, FCM is still one of the most popular clustering methods, due to its partition quality and its easily understandable and implementable alternating optimization (AO) solution. This is happening in spite of the facts that FCM was found sensitive to outliers [29], and sometimes it converges quite slowly [31]. The sensitivity to outliers was avoided by relaxing the probabilistic constraint. After an early solution given by Davé [33] (which later was further developed by Menard et al. [34]), Krishnapuram and Keller came up with the possibilistic *c*-means algorithm (PCM), which distributes the partition matrix elements based on statistical rules. The degrees of memberships are not anymore probabilities. Instead of that, they describe the compatibility of input data with different clusters. The compatibility of item c with cluster number i only depends on the distance between them, and the previously established penalty term η_i. The possibilistic approach represented an instant solution for the sensitivity to outliers, but several new problems emerged. The fact that PCM distributes typicality values independently of each other often leads to coincident clusters [29].

In order to avoid the coincidence of possibilistic cluster prototypes, several solutions have been proposed [35,36], which culminated in the so-called possibilistic-fuzzy *c*-means (PFCM) clustering model by Pal et al. [30]. After a long series of tests using standard data sets, the authors found PFCM a reliable robust clustering scheme, and recommended giving the possibilistic component a higher weight within the mixture and setting the fuzzy exponent m greater than the possibilistic exponent p.

On the other hand, Fan et al. [31] introduced the suppressed FCM algorithm (s-FCM), having the intention of combining the quicker convergence of HCM with the accurate partitioning properties of FCM. They added an extra computation step into the FCM iteration, which created a competition among clusters: after performing the computation of fuzzy memberships, low membership values are suppressed via multiplication with a previously defined suppression rate $\alpha \in [0,1]$, and the largest membership is raised by swallowing all the suppressed parts of the low memberships, retaining the probabilistic constraint. Cluster prototypes are then updated with FCM's formula using the modified fuzzy memberships. This algorithm is able to reduce FCM's computational load, and with a carefully chosen suppression rate and intelligent distribution of initial cluster prototype, it can reliably achieve fine partitions. Although s-FCM is not an optimal algorithm [32], it had a considerable contribution to quick *c*-means clustering based partitioning.

2.2. INU compensation models

The conventional *c*-means clustering models classify the set of data $\{x_k\}$, which was recorded among ideal circumstances, containing no noise. However, in the real case, the observed data $\{y_k\}$ differs from the actual one $\{x_k\}$: there are impulse and Gaussian noises that can be handled with a smart prefiltering, and there is the intensity non-uniformity (INU) artefact, which needs to be compensated during segmentation.

Literature recommends three different data variation models for intensity inhomogeneity. The bias field model considers INU as an additive noise: for each pixel k we have $y_k = x_k + b_k$, where b_k represents the bias value at pixel k [1,15,25]. The gain field model describes INU as a multiplicative field, having a gain value g_k for each pixel k, such that $y_k = g_k x_k$ [37]. The so-called log bias approach in fact is a gain field estimation reduced to bias computation using the logarithmic formula $\log y_k = \log g_k + \log x_k$ [24].

Regardless of the applied compensation model, the variation of the intensity between neighbor pixels has to be slow. Zero gradient conditions derived from the quadratic objective functions do not produce such estimations. Consequently, a smoothing operation is necessary to assure this slow variation of the estimated bias or gain field.

3. Materials and methods

3.1. The proposed hybrid clustering model

In this section we propose a hybrid c-means clustering model, which consists of a linear combination of the hard, fuzzy, and possibilistic criteria. The cost function of such a model is:

$$J_{\text{hyb}} = \beta\alpha J_{\text{FCM}} + (1-\beta)J_{\text{PCM}} + \beta(1-\alpha)J_{\text{HCM}}, \tag{1}$$

or more explicitly

$$J_{\text{hyb}} = \sum_{k=1}^{n}\sum_{i=1}^{c}\xi_{ik}||x_k - v_i||^2 + (1-\beta)\sum_{i=1}^{c}\eta_i\sum_{k=1}^{n}(1-t_{ik})^p, \tag{2}$$

where $\xi_{ik} = [\beta\alpha u_{ik}^m + (1-\beta)t_{ik}^p + \beta(1-\alpha)h_{ik}]$ is the mixed partition matrix element describing the degree to which the input item x_k is assigned to cluster index i; h_{ik}, u_{ik}, and t_{ik} represent the degrees of membership of input datum x_k with respect to cluster C_i, assigned by the hard, fuzzy, and possibilistic criteria, respectively, constrained by $h_{ik} \in \{0,\ 1\}$, $\sum_{i=1}^{c} h_{ik} = 1\ \forall k = 1 \ldots n$; $u_{ik} \in [0,\ 1]$, $\sum_{i=1}^{c} u_{ik} = 1\ \forall k = 1 \ldots n$; $t_{ik} \in [0,\ 1]$, $0 < \sum_{i=1}^{c} t_{ik} < c\ \forall k = 1 \ldots n$, and $0 < \sum_{k=1}^{n} t_{ik} < n\ \forall i = 1 \ldots c$; m and p are the exponents of the fuzzy and possibilistic terms, restricted by $m > 1$ and $p > 1$, as defined in [27] and [28], respectively; η_i, $i = 1 \ldots c$, are the variance parameters of the possibilistic term defined as

$$\eta_i = \kappa \cdot \frac{\sum_{k=1}^{n} u_{ik}^m ||x_k - v_i||^2}{\sum_{k=1}^{n} u_{ik}^m} \tag{3}$$

[28]; α and β are tradeoff parameters, constrained by $0 \le \alpha \le 1$ and $0 \le \beta \le 1$, which control the relative strength of the three terms within the hybrid cost function. In this order, β controls the strength of possibilistic clustering, while α is responsible of the FCM-HCM ratio in the mixture, similarly to the case of suppressed FCM. Fig. 1 shows some special cases of the tradeoff parameters: these only cover the most part of the boundary and the three corners of the domain of definition.

The AO iterative solution scheme is obtained using zero gradient conditions and Lagrange multipliers. Not at all surprisingly, the partition update formulas are obtained exactly as in the conventional HCM, FCM, and PCM algorithms. For any $i = 1 \ldots c$ and $k = 1 \ldots n$, we get:

$$h_{ik} = \begin{cases} 1 & \text{if } i = \arg\min_j \{||x_k - v_j||, j = 1 \ldots c\} \\ 0 & \text{otherwise} \end{cases}, \tag{4}$$

$$u_{ik} = \frac{\sqrt[m-1]{||x_k - v_i||^{-2}}}{\sum_{j=1}^{c} \sqrt[m-1]{||x_k - v_j||^{-2}}}, \tag{5}$$

$$t_{ik} = \left(1 + \sqrt[p-1]{\frac{||x_k - v_i||^2}{\eta_i}}\right)^{-1}. \tag{6}$$

The cluster prototype update formula, which also comes from the zero gradient conditions, will have the following form:

$$v_i = \frac{\sum_{k=1}^{n}[\beta\alpha u_{ik}^m + (1-\beta)t_{ik}^p + \beta(1-\alpha)h_{ik}]x_k}{\sum_{k=1}^{n}[\beta\alpha u_{ik}^m + (1-\beta)t_{ik}^p + \beta(1-\alpha)h_{ik}]}. \tag{7}$$

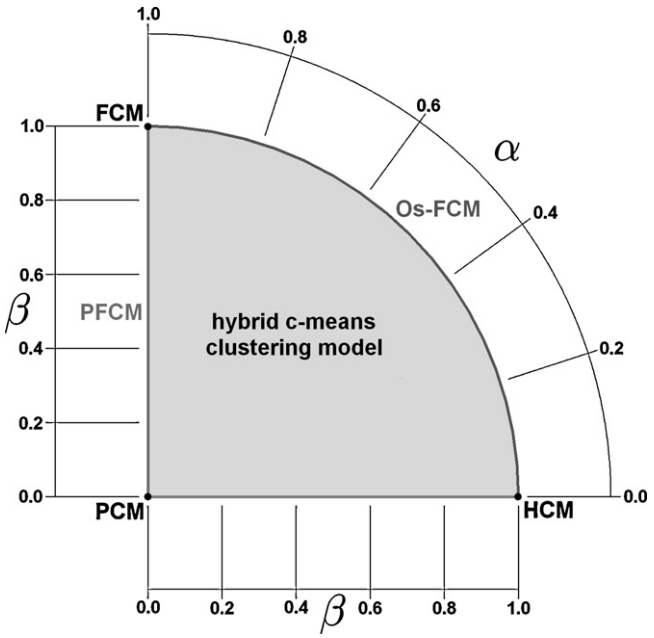

Fig. 1. Parametrization of the proposed hybrid clustering model, its domain of definition with special cases at the boundary and corners: $\beta = 0$ corresponds to PCM, $\beta = 1$ and $\alpha = 0$ is HCM, $\beta = 1$ and $\alpha = 1$ reduces to FCM, $\alpha = 1$ and $\beta \in (0, 1)$ is the PFCM model of Pal et al. [30], and finally $\beta = 1$ and $\alpha \in (0, 1)$ is the optimally suppressed FCM (Os-FCM) introduced in [32].

Similarly to the AO scheme of the FCM algorithm, the partition update formulas (4)–(6), and the prototype update rule (7) are repeatedly applied until cluster prototypes stabilize.

3.2. The proposed INU compensation schemes

In the following, we will combine the hybrid c-means clustering algorithm with the INU modeling schemes, in order to segment heavily INU-contaminated MR brain images. Pixels of such images are characterized by a single feature value representing the observed intensity of the pixel. Under such circumstances, using bias field for INU compensation, the modified objective function becomes:

$$J_{\text{hyb-b}} = \sum_{k=1}^{n}\sum_{i=1}^{c}\xi_{ik}(y_k - b_k - v_i)^2 + (1-\beta)\sum_{i=1}^{c}\eta_i\sum_{k=1}^{n}(1-t_{ik})^p. \tag{8}$$

On the other hand, if we approximate the INU artefact as a gain field, the objective function is:

$$J_{\text{hyb-g}} = \sum_{k=1}^{n}\sum_{i=1}^{c}\xi_{ik}(y_k - g_k v_i)^2 + (1-\beta)\sum_{i=1}^{c}\eta_i\sum_{k=1}^{n}(1-t_{ik})^p. \tag{9}$$

Both approaches use the same hybrid partition ξ_{ik}, which on its turn depends on the tradeoff parameters α and β, as shown in Fig. 1. Both modified objective functions are optimized using the zero gradient conditions. The computation of the fuzzy partitions also requires the use of Lagrange multipliers. The optimization formulas are presented in Table 1, while details showing the way they were obtained are revealed in Appendix A.

The estimation process of the bias or gain field does not assure a smooth variation of the INU. In fact, the fuzzy and hard component of the cost function are strongly pushed towards 0 with specially chosen b_k or g_k values, in the following way:

1. For any observed intensity value y_k, we can choose a winner cluster prototype v_{w_k} (e.g. $w_k = \arg\min_i(|y_k - b_k - v_i|)$, and solv-

Table 1
Optimization formulas of the modified cost function of the hybrid *c*-means clustering model, aiming at INU correction via bias and gain field estimation.

Formula	Bias field approach	Gain field approach
(A) Fuzzy partition	$u_{ik} = \frac{\sqrt[m-1]{(y_k - b_k - v_i)^{-2}}}{\sum_{j=1}^{c} \sqrt[m-1]{(y_k - b_k - v_j)^{-2}}}$	$u_{ik} = \frac{\sqrt[m-1]{(y_k - g_k v_i)^{-2}}}{\sum_{j=1}^{c} \sqrt[m-1]{(y_k - g_k v_j)^{-2}}}$
(B) Possibilistic partition	$t_{ik} = \left[1 + \sqrt[p-1]{\frac{(y_k - b_k - v_i)^2}{\eta_i}}\right]^{-1}$	$t_{ik} = \left[1 + \sqrt[p-1]{\frac{(y_k - g_k v_i)^2}{\eta_i}}\right]^{-1}$
(C) Hard partition	$h_{ik} = \begin{cases} 1 & \text{if } i = \arg\min_j \{\lvert y_k - b_k - v_j \rvert\} \\ 0 & \text{otherwise} \end{cases}$	$h_{ik} = \begin{cases} 1 & \text{if } i = \arg\min_j \{\lvert y_k - g_k v_j \rvert\} \\ 0 & \text{otherwise} \end{cases}$
(D) Hybrid partition	$\xi_{ik} = \beta\alpha u_{ik}^m + (1-\beta) t_{ik}^p + \beta(1-\alpha) h_{ik}$	$\xi_{ik} = \beta\alpha u_{ik}^m + (1-\beta) t_{ik}^p + \beta(1-\alpha) h_{ik}$
(E) Cluster prototypes	$v_i = \frac{\sum_{k=1}^{n} \xi_{ik}(y_k - b_k)}{\sum_{k=1}^{n} \xi_{ik}}$	$v_i = \frac{\sum_{k=1}^{n} \xi_{ik} g_k y_k}{\sum_{k=1}^{n} \xi_{ik} g_k^2}$
(F) INU field estimation	$b_k = y_k - \frac{\sum_{i=1}^{c} \xi_{ik} v_i}{\sum_{i=1}^{c} \xi_{ik}}$	$g_k = y_k \cdot \frac{\sum_{i=1}^{c} \xi_{ik} v_i}{\sum_{i=1}^{c} \xi_{ik} v_i^2}$

ing ties arbitrarily), and set $b_k = y_k - v_{w_k}$. With this bias value we get $u_{w_k k} = h_{w_k k} = 1$, and $u_{ik} = h_{ik} = 0$ for any $i \neq w_k$. If we repeat this procedure for all pixels, two of the three components of the cost function will reduce to zero.

2. Similarly at gain field estimation, we can choose $g_k = y_k / v_{w_k}$, which yields $u_{w_k k} = h_{w_k k} = 1$, and $u_{ik} = h_{ik} = 0$ for any $i \neq w_k$, obviously zeroing the above mentioned two components.

However, none of these trivial minima serve the smoothness of the estimated INU field. In order to avoid this shortcoming, besides using a strong possibilistic component in the hybrid partition, a smoothing filter is employed at the end of each iteration, which determine the b_k or g_k values to follow the slow variation of the inhomogeneity.

3.3. Image filtering

In order to assure the robustness of the proposed segmentation algorithm, two context dependent filters are employed. The first one, applied as a prefiltering before segmentation, serves the elimination of high-frequency noises from the input image. The second filtering technique is involved in the INU compensation and assures the smooth variation of the estimated bias or gain field.

Impulse and Gaussian noises are removed from the original MR image using a context dependent local filtering, which combines averaging and median filtering effects based on physical distances and gray level differences between neighbor pixels. The filter was presented in details in our previous work [38].

The intensity inhomogeneity artefact varies slowly along the image. This property is ignored by both compensation approaches presented above: the estimated bias or gain field does contain tissue details. To avoid this problem, a filtering step is necessary in each computation cycle, after having computed the bias or gain field, to smoothen the estimated field and thus eliminate the high-frequency components that mainly correspond to tissue details.

The smoothing filter has to be designed in a way that it conforms to the following warnings. If the size of the filter mask is too large, the filter will be too strong: it will not only eliminate tissue patterns from the bias or gain value, but also will suppress the estimated inhomogeneity, leading to failed segmentation. On the other hand, if the size of the filter mask is too small, the filter will be too weak to eliminate all tissue patterns. In this case, the edges in the compensated image will lose their sharpness, leading to several misclassifications along the tissue boundaries.

Most INU compensation approaches, not only those using *c*-means clustering, apply large sized averaging filters, with window sizes varying from 11×11 to 31×31 pixels. These filters are performed once or more times in each cycle [4]. In order to deal with the above mentioned warnings, in a previous work [37] we proposed a context sensitive smoothing filter that performs a repeated averaging in every iteration, where the number of repetitions are locally decided using a morphological criterion. The main parameters of this smoothing filter is the shape and size of the morphological structuring element, and the mask size of the averaging filter.

A further enhancement of this smoothing process is achieved by allowing the averaging mask of the smoothing filter to change its size and shape, according to local conditions. The main local properties of the smoothed bias or gain field, which affect the mask parameters, are the gradient strength and direction. In the first iteration of the hybrid *c*-means algorithm, smoothing uses a predefined square shaped mask called basic mask. In any further iteration, the gradient strength and direction of the smoothed bias or gain field computed in the previous iteration, determine the deformation of the locally applied averaging mask. Higher gradient components require stronger averaging, so they imply a deformed, rectangular shaped mask, longer in the direction of the gradient vector.

Another important step of the smoothing is to shift the bias (gain) values in order to assure the zero-mean (1-mean) value. Neglecting this effect may distort the cluster prototype intensities.

3.4. Multiple stage bias and gain field estimation

Bias or gain field estimation using the previous FCM-based approaches [1,25] can only handle the INU artefact to a limited amplitude. For any pixel, the *c*-means clustering algorithm assigns the highest degree of membership to the closest cluster. Consequently, when the INU amplitude is comparable with the distance between clusters, these pixels will be attracted by the wrong cluster, and the bias or gain field will be estimated accordingly. The smoothing of the bias and gain field may repair this kind of misclassifications, but the larger these wrongly labeled spots are, the harder it will be to eliminate them via smoothing.

In order to deal with high-amplitude INU artefacts, we propose performing the bias or gain field estimation in multiple stages. When the modified hybrid *c*-means algorithm using the optimization formulas from either column of Table 1 has converged, we modify the input (observed) image according to the estimated bias or gain field:

$$y_k = y_k^{(\text{old})} - b_k \quad \text{or} \quad y_k = \frac{y_k^{(\text{old})}}{g_k}, \tag{10}$$

and then restart the algorithm from the beginning, using the modified input image.

3.5. The proposed segmentation algorithm

The presented algorithm can be summarized as follows:

1. Remove the Gaussian and impulse noises from the MR image using the context dependent prefiltering technique proposed in [38].
2. Set initial parameters of the hybrid clustering model, including tradeoff parameters α and β, fuzzy and possibilistic exponents m and p, and the possibilistic penalty terms η_i.
3. Initialize cluster prototypes v_i, $i = 1 \ldots c$, with random values differing from each other.
4. Initialize the bias (gain) field values with 0-mean (1-mean) random numbers having reduced variance, or simply set $b_k = 0$ ($g_k = 1$) for all pixels.
5. Compute the new fuzzy partition values u_{ik}, $i = 1 \ldots c$, $k = 1 \ldots n$, using the corresponding formula indicated in Table 1, row (A).
6. Compute the new possibilistic partition values t_{ik}, $i = 1 \ldots c$, $k = 1 \ldots n$, using the corresponding formula indicated in Table 1, row(B).
7. Compute the new hard partition values h_{ik}, $i = 1 \ldots c$, $k = 1 \ldots n$, using the corresponding formula indicated in Table 1, row (C).
8. Build up the new hybrid partition, based on the tradeoff parameter values α and β, as indicated in Table 1, row (D).
9. Compute new cluster prototype values v_i, $i = 1 \ldots c$, using the corresponding formula indicated in Table 1, row (E).
10. Perform new bias or gain field estimation for each pixel k using the corresponding formula indicated in Table 1, row (F).
11. Smoothen the bias or gain field using the proposed smoothing filter, using the context dependent filtering technique proposed in Section 3.3.
12. Repeat steps 5–11 until there is no relevant change in the cluster prototypes. This is tested by comparing any norm of the difference between the new and the old vector $\mathbf{v}$ with a preset small constant ε.
13. Modify the input image according to the estimated bias or gain field using (10), and repeat steps 3–12 until the INU artefact is compensated. The algorithm usually requires a single repetition.

We can observe that steps 5–7 do not depend on each other, so they can be computed in any order, or even they can be performed by parallel tasks. The order shown here was chosen arbitrarily.

4. Results and discussion

4.1. Validation of the clustering model

The proposed hybrid c-means clustering model has undergone thorough validation process, using several standard test data sets including the Iris data [39] and the Wine data [40]. The main properties of these two data sets are summarized in Table 2. Iris data represents a collection of 150 feature vectors containing 4 different measures of individual iris flowers. Wine data comprises 13 well defined chemical parameters of 178 different wines. The vectors in both data sets belong to three different classes, as indicated by the labels assigned to each vector. Classes in Iris data have 50 items each, while Wine classes have unequal cardinalities. The parameters in the Wine data set have wide and various ranges; that is why these vectors have to be normalized before clustering. Iris sizes do not vary to much, so their normalization is not necessary.

Table 2
Properties of the most popular test data sets.

Property	Iris data	Wine data
Feature vectors	150	178
Dimensions	4	13
Classes	3	3
Cardinality of classes	50, 50, 50	59, 71, 48
Normalization	Optional	Mandatory
Correct decisions with FCM	Approx. 134	Approx. 169
Acceptable MCR	11%	5%

Table 3
The best accuracy achieved using the hybrid c-means clustering model.

Accuracy criterion	Iris data	Wine data
Minimum correct decisions	139	171
Maximum correct decisions	140	172
Average correct decisions	139.72	171.65
Average MCR	6.85%	3.57%

In the Iris data set, one class is well separated from the other two, but these latter ones seriously overlap each other. That is why, a misclassification rate (MCR) of 10–11% in case of the Iris data is acceptable. On the other hand, conventional clustering algorithms provide 4–5% of misclassifications on the normalized Wine data set.

As a first part of the evaluation of the proposed hybrid c-means algorithm, we have analyzed the influence of the system parameters (α, β, κ, m, p) upon the MCR value. The whole domain of definition of tradeoff parameters α and β was tested at resolutions of 0.001–0.025. For each setting, the hybrid clustering was performed 200 times using predefined sets of randomly chosen initialization of the cluster prototypes. The main criterion of accuracy was the MCR averaged over the 200 runs. Details on the best achieved accuracy are shown in Table 3. These numeric values show the superiority of the well tuned hybrid approach over FCM.

Fig. 2 exhibits the classification accuracy plotted against α and β, using variance penalty terms η_i conditioned by $\kappa = 1$. The left part of the figure shows the whole domain of definition of the tradeoff parameters, while the right part magnifies those areas where higher accuracy was obtained. Using higher values of κ has two visible consequences:

1. the areas of highest accuracy drift outwards within the sector of the circle;
2. the best achieved MCR slightly rises.

This latter effect and the recommendations given in [28] determined us to use $\kappa = 1$ in all further tests.

The convergence speed of the algorithm, characterized by the average number of iterations that are necessary to obtain a certain stability of cluster prototypes, has also been tested in the whole domain of tradeoff parameters. Tests have revealed the deterministic presence of a critical point along the axis $\alpha = 1$, generally situated in the interval $\beta \in [0.1, 0.15]$, indicating that a dominantly possibilistic mixture, which is free from HCM component, is likely to need significantly more iterations than any other hybrid mixture. In the proximity of this point, hybrid clustering may require hundreds of iterations to reach convergence, which is an undesired phenomenon. Consequently, tradeoff parameters have to be chosen such a way to avoid this critical point.

Cluster validity has been tested using an easily implementable and comprehensible cluster validity index (CVI): $\mathrm{CVI} = \min\{||v_i - v_j|| : 1 \le i < j \le c\}$, which represents the minimum distance between any pair of cluster prototypes. We call a solution stable or valid if its CVI is high, and unstable or invalid if its CVI is low. Thorough test have revealed that pure PCM and mixtures situated close to PCM (conditioned by $\beta < 0.1$) have significantly lower stability than any other mixture.

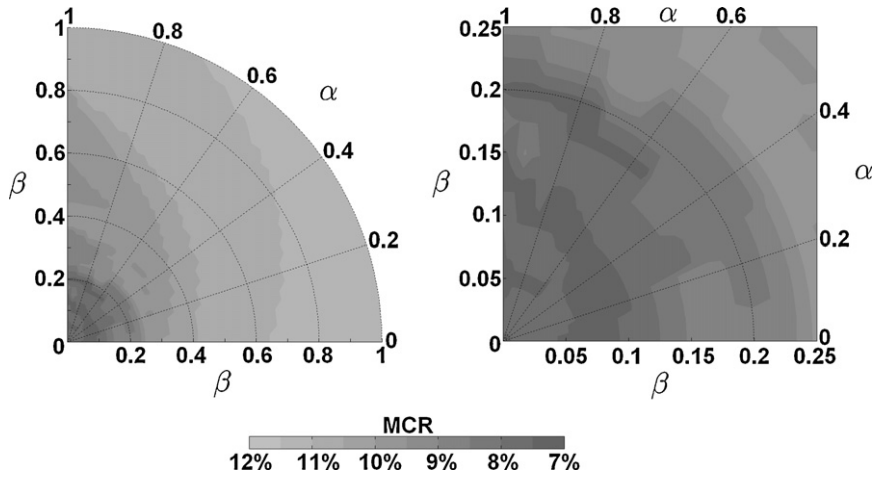

Fig. 2. The average accuracy of the Iris data partitions, plotted against tradeoff parameters α and β, using possibilistic penalty terms η_i conditioned by $\kappa = 1$. The right graph shows a magnified view of the region bounded by $\beta < 0.25$.

Finally, let us summarize the recommendation regarding tradeoff parameters:

1. The possibilistic penalty terms should be computed using $\kappa = 1$, to ensure our chances to achieve the best possible accuracy;
2. Setting $\beta \in [0.1, 0.15]$ keeps us far enough from pure PCM and ensures low sensibility to outlier data;
3. Setting $\alpha \in [0.25, 0.75]$ avoids the critical point of convergence speed. Lower α values make the convergence quicker, but may also have bad influence upon accuracy.

These parameter settings ensure the robustness of the classification process and provide fine partitions regardless on the initial cluster prototypes. For further details regarding the

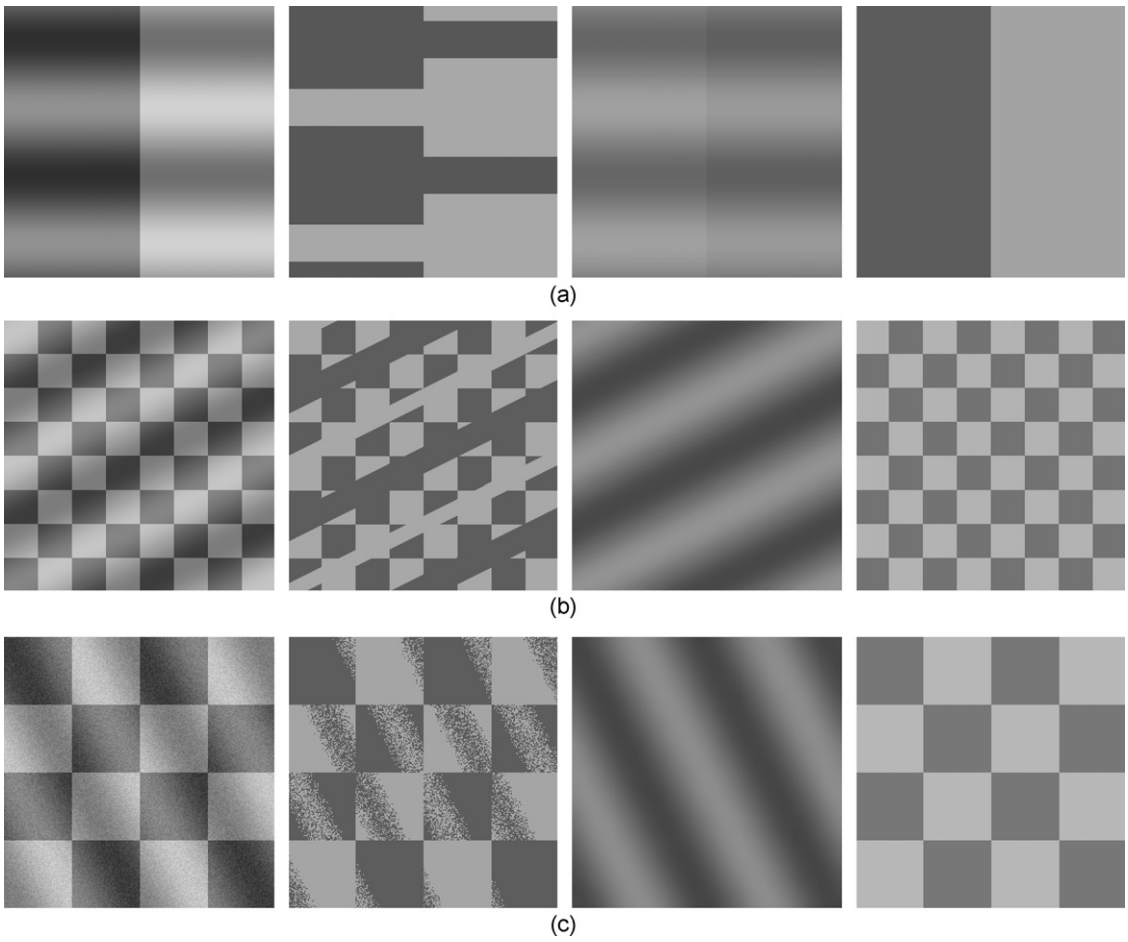

Fig. 3. Inhomogeneity correction using three different phantoms: the first column in each row shows the original image, the second presents the failed FCM-based segmentation without INU compensation, the third column exhibits the estimated bias field, while the last column shows the final segmentation result. Row (c) treats the case when an amount of high-frequency noise is also present.

validation of the clustering model, the reader is referred to [41].

4.2. Image segmentation experiments

We applied the presented filtering, INU compensation and image segmentation techniques to several phantoms and T1-weighted real MR images taken from the Internet Brain Segmentation Repository [42], artificially contaminated with different kinds of noises. The distance between neighbor pixels in all real images involved in this test were between 0.8 and 1.0 mm. According to the recommendations formulated in the previous section, the tradeoff parameters of the hybrid clustering model were set to $\alpha = 0.5$, $\beta = 0.1$, and $\kappa = 1$.

The proposed inhomogeneity compensation method was tested on both artificial phantoms and real MR images. Brain MR images are segmented to three classes: white matter, gray matter, and cerebrospinal fluid. Most phantoms used for testing had two or three relevant intensity classes. The results of bias and gain field estimation performed on phantom images are shown in Fig. 3. The conventional FCM or the hybrid clustering model without compensation cannot handle the INU artefact correctly, but with the use of smoothed bias or gain field estimation, this phenomenon is efficiently overcome. The compensation succeeded in one stage, and provided the same accuracy for both the bias and the gain field approach.

In case of low-amplitude inhomogeneity, a single stage of bias or gain field estimation is sufficient for real MR images as well. However, as the magnitude of the INU rises, more stages will be necessary to produce an acceptable segmentation. Fig. 4 shows the intermediary and final results of a segmentation process, performed on a heavily INU-contaminated MR image. The inhomogeneity correction succeeds after two stages. Although most of the non-uniformity present in the input image is compensated in the first stage, the remaining part still makes the FCM or hybrid clustering based segmentation fail, so a second stage is necessary. After the second stage, the compensated image seems to have preserved the sharpness of its edges, which is necessary for an accurate segmentation.

Several tests on T1-weighted real images contaminated with high-magnitude INU were performed, using:

1. different fixed sizes and shapes of the structuring element of the proposed morphological smoothing filter, and
2. a set of smoothing windows, with sizes ranging from 9×9 to 31×31.

The evaluation using real MR images was performed using 45 different, T1 weighted MR brain images from various healthy patients. The proposed algorithm with various settings was tested to segmentation all images, and the MCR was averaged for each setting. Table 4 gives an insight into the best averaged misclassification percentages obtained in various circumstances. For each given setting of the morphological filter, the best obtained average MCR is given, together with the averaging window size, for both the FCM-based, and the hybrid clustering based segmentation methods. The last column reports the MCR obtained using the hybrid approach and the adaptive averaging window size. The most relevant facts reflected by this table are:

1. If the averaging window size is fixed, the most accurate segmentation is obtained at a window size of 17×17 or 19×19 pixels. This is why, for the adaptive windowed averaging, we recommend using one of these as initial setting.
2. The hybrid clustering model always produces better accuracy with respect to the FCM-based approach. Using the hybrid approach instead of the fuzzy partitioning reduces the MCR by 17.07% in average.

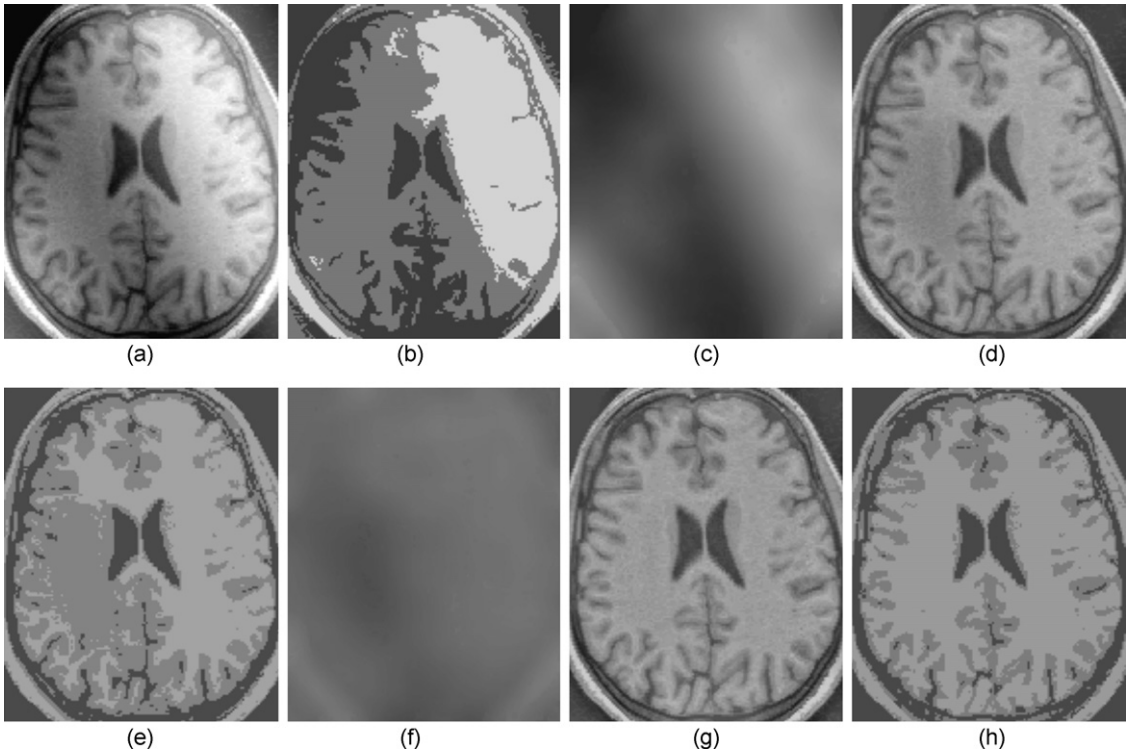

Fig. 4. Segmentation of a heavily inhomogeneous real MR image: (a) original, (b) segmentation without compensation, (c) bias field estimated in the first stage, (d) compensated MR image after first stage, (e) FCM-based segmentation after first stage, still unusable, (f) bias field estimated in the second stage, (g) final compensated image, (h) segmented image.

Table 4
Misclassification percentages with various smoothing filters, in case of heavily INU-contaminated MR images. The first filter is simple averaging, while all others contain the proposed morphological criterion. The adaptive mask had an initial size of 17×17 pixels.

Structuring element		Fuzzy c-means model		Hybrid c-means model		
Size	Shape	MCR	Mask size	MCR	Mask	MCR with adaptive mask
Averaging	None	4.368%	17×17	3.795%	19×19	3.381%
3×3	Square	2.852%	17×17	2.428%	17×17	2.297%
5×5	Cross	3.561%	19×19	2.856%	19×19	2.389%
7×7	Cross	3.309%	19×19	2.962%	19×19	2.523%
11×11	Cross	3.268%	19×19	2.807%	17×17	2.422%

3. The adaptive sized smoothing window can bring another 14.15% improvement of the misclassification rate.
4. The most accurate partitions were obtained using 3×3 square or 5×5 pixel cross shaped structuring element and adaptive smoothing window.
5. The obtained MCR values are at the same level as the best reported ones in the literature of INU compensation [4].

The color of tumors in MR images usually differs from WM, GM, and CSF. That is why, when one wants to segment an image with tumor, the number of classes should be set to $c = 4$.

Using several repetitive stages during INU compensation may reduce the intensity difference between tissue classes, leading to misclassifications. That is why the estimation is limited to two steps, performing several stages is not recommendable. However, in case of T1-weighted brain MR images and segmentation into three clusters, no more than two stages are necessary.

Although the bias- and gain field compensation approaches differ in their formulation, there is no significant difference between their efficiency and accuracy, that is, there is no evidence for any of them to be superior.

The classification accuracy of the proposed algorithm is slightly better than those of reported FCM-based INU compensation methods [1,25]. The major superiority of the proposed method consists in the fact, that in case of high-amplitude INU artefact, most of the reported methods fail at the point indicated in Fig. 4(d) and (e).

The usage of the hybrid clustering model instead of the FCM algorithm does not mean a relevant extra computational load. Although the duration of an iteration in the internal loop (steps 5–11 of the algorithm given in Section 3.5) rises by 18–20%, the number of necessary iterations to reach convergence falls about the same amount, making the total duration of the segmentation approximately equal to that of the FCM algorithm. This is why the proposed method performs about in the same time as the intelligent modified FCM based algorithm of Siyal and Yu [1], and is quicker than the BCFCM [25] by an order of magnitude, as this latter uses a computationally costly in-loop regularizer operation.

The computations performed by the proposed algorithm can be easily scheduled to parallel execution, significantly reducing the execution time. Parallelized execution may be implemented on either multi-processor systems or modern graphical processing units.

5. Conclusion

A novel method has been proposed for the segmentation of MR images in the presence of intensity non-uniformity. The proposed approach replaces the key element of the conventional FCM-based INU compensation, involving a hybrid c-means algorithm into the partitioning process. Further on, a new adaptive smoothing filter has been proposed to assist the bias or gain field estimation embedded into the hybrid c-means based algorithmic scheme.

The hybrid c-means clustering algorithm was validated using widely used test data sets. The optimal tradeoff parameters were extracted in order to support fine partitioning.

The proposed image segmentation method proved to produce accurate partitions in the presence of severe intensity non-uniformity. The quantitative evaluation of the segmentation quality revealed the superiority of the well-tuned hybrid c-means algorithm over FCM, and placed the proposed method among the most accurate segmentation techniques in the presence of high-magnitude INU artifacts.

Acknowledgments

This work was supported by CNCSIS-UEFISCSU, project number PN II-RU PD 667/2010.

Appendix A. Details on the optimization of the modified hybrid objective functions

A.1. Bias field estimation formulas

In the bias field based INU estimation approach, the modified cost function is given as:

$$\begin{aligned}\mathcal{L}_{\text{bias}} &= J_{\text{hyb-b}} + \sum_{k=1}^{n}\lambda_k \sum_{i=1}^{c}\left(1 - \sum_{i=1}^{c} u_{ik}\right) \\ &= \sum_{i=1}^{c}\sum_{k=1}^{n}[\beta\alpha u_{ik}^{m} + (1-\beta)t_{ik}^{p} + \beta(1-\alpha)h_{ik}](y_k - b_k - v_i)^2 \,, \\ &\quad + (1-\beta)\sum_{i=1}^{c}\eta_i \sum_{k=1}^{n}(1-t_{ik})^p + \sum_{k=1}^{n}\lambda_k \sum_{i=1}^{c}\left(1 - \sum_{i=1}^{c} u_{ik}\right)\end{aligned}$$

where λ_k, $k = 1 \ldots n$ are the Lagrange multipliers. Let us start the investigation of the zero gradient conditions we can get from the partial derivatives with respect to fuzzy memberships u_{ik}.

$$\frac{\partial L_{\text{bias}}}{\partial u_{ik}} = 0 \quad \Rightarrow \quad m\alpha\beta u_{ik}^{m-1}(y_k - b_k - v_i)^2 = \lambda_k,$$

which in case of $\alpha\beta \neq 0$ becomes

$$u_{ik} = \sqrt[m-1]{\frac{\lambda_k}{m\alpha\beta}} \cdot \sqrt[m-1]{(y_k - b_k - v_i)^{-2}}$$

The probabilistic constraint of fuzzy memberships implies:

$$\sum_{j=1}^{c} u_{jk} = 1 \quad \Rightarrow \quad \sqrt[m-1]{\frac{\lambda_k}{m\alpha\beta}} = \left(\sum_{j=1}^{c}\sqrt[m-1]{(y_k - b_k - v_j)^{-2}}\right)^{-1},$$

and consequently we get

$$u_{ik} = \frac{\sqrt[m-1]{(y_k - b_k - v_i)^{-2}}}{\sum_{j=1}^{c}\sqrt[m-1]{(y_k - b_k - v_j)^{-2}}}.$$

With respect to h_{ik}, the cost function cannot be differentiated. Hard partition is established using the winner-takes-all rule.

The update formula of the possibilistic partition is obtained as follows:

$$\frac{\partial J_{\text{hyb-b}}}{\partial t_{ik}}=0 \quad \Rightarrow \quad p(1-\beta)t_{ik}^{p-1}(y_k-b_k-v_i)^2=p(1-\beta)\eta_i(1-t_{ik}^{p-1}),$$

which in case of $\beta \neq 1$ implies

$$\frac{(y_k-b_k-v_i)^2}{\eta_i}=\left(\frac{1}{t_{ik}}-1\right)^{p-1} \Rightarrow t_{ik}=\left[1+\sqrt[p-1]{\frac{(y_k-b_k-v_i)^2}{\eta_i}}\right]^{-1}.$$

Let us remark here that in case of $\alpha\beta=0$ the fuzzy term is not present in the hybrid, while in case of $\beta=1$ the possibilistic term is absent, so their optimization can be neglected. This property is also valid in case of the gain field approach, presented in the next section.

The update formula of cluster prototypes comes from the zero gradient condition

$$\frac{J_{\text{hyb-b}}}{\partial v_i}=0 \quad \Rightarrow \quad -2\sum_{k=1}^{n}\xi_{ik}(y_k-b_k-v_i)=0,$$

which implies

$$\sum_{k=1}^{n}\xi_{ik}(y_k-b_k)=v_i\sum_{k=1}^{n}\xi_{ik} \quad \Rightarrow \quad v_i=\frac{\sum_{k=1}^{n}\xi_{ik}(y_k-b_k)}{\sum_{k=1}^{n}\xi_{ik}}.$$

Finally, we need to partially differentiate the cost function with respect to b_k:

$$\frac{\partial J_{\text{hyb-b}}}{\partial b_k}=0 \quad \Rightarrow \quad -2\sum_{i=1}^{c}\xi_{ik}(y_k-b_k-v_i)=0,$$

which leads to

$$(y_k-b_k)\sum_{i=1}^{c}\xi_{ik}=\sum_{i=1}^{c}\xi_{ik}v_i \quad \Rightarrow \quad b_k=y_k-\frac{\sum_{i=1}^{c}\xi_{ik}v_i}{\sum_{i=1}^{c}\xi_{ik}}.$$

A.2. Gain field estimation formulas

Lagrange multipliers make the cost function of the gain field approach look like:

$$\begin{aligned}\mathcal{L}_{\text{gain}} &= J_{\text{hyb-g}}+\sum_{k=1}^{n}\lambda_k\sum_{i=1}^{c}\left(1-\sum_{i=1}^{c}u_{ik}\right)\\ &=\sum_{i=1}^{c}\sum_{k=1}^{n}[\beta\alpha u_{ik}^{m}+(1-\beta)t_{ik}^{p}+\beta(1-\alpha)h_{ik}](y_k-g_kv_i)^2\\ &\quad+(1-\beta)\sum_{i=1}^{c}\eta_i\sum_{k=1}^{n}(1-t_{ik})^p+\sum_{k=1}^{n}\lambda_k\sum_{i=1}^{c}\left(1-\sum_{i=1}^{c}u_{ik}\right)\end{aligned},$$

where $\lambda_k, k=1\ldots n$ are the Lagrange multipliers. The partial derivatives with respect to fuzzy memberships u_{ik} will be

$$\frac{\partial L_{\text{gain}}}{\partial u_{ik}}=0 \quad \Rightarrow \quad m\alpha\beta u_{ik}^{m-1}(y_k-g_kv_i)^2=\lambda_k,$$

which in case of $\alpha\beta \neq 0$ becomes

$$u_{ik}=\sqrt[m-1]{\frac{\lambda_k}{m\alpha\beta}}\cdot\sqrt[m-1]{(y_k-g_kv_i)^{-2}}.$$

The probabilistic constraint of fuzzy membership implies:

$$\sum_{j=1}^{c}u_{jk}=1 \quad \Rightarrow \quad \sqrt[m-1]{\frac{\lambda_k}{m\alpha\beta}}=\left(\sum_{j=1}^{c}\sqrt[m-1]{(y_k-g_kv_j)^{-2}}\right)^{-1}$$

so consequently we get

$$u_{ik}=\frac{\sqrt[m-1]{(y_k-g_kv_i)^{-2}}}{\sum_{j=1}^{c}\sqrt[m-1]{(y_k-g_kv_j)^{-2}}}.$$

The update formula of the possibilistic partition is obtained as follows:

$$\frac{\partial J_{\text{hyb-g}}}{\partial t_{ik}}=0 \quad \Rightarrow \quad p(1-\beta)t_{ik}^{p-1}(y_k-g_kv_i)^2=p(1-\beta)\eta_i(1-t_{ik}^{p-1}),$$

which in case of $\beta \neq 1$ implies

$$\frac{(y_k-g_kv_i)^2}{\eta_i}=\left(\frac{1}{t_{ik}}-1\right)^{p-1} \quad \Rightarrow \quad t_{ik}=\left[1+\sqrt[p-1]{\frac{(y_k-g_kv_i)^2}{\eta_i}}\right]^{-1}.$$

Similarly to the bias estimation case, hard partition is established using the winner-takes-all rule.

The update formula of cluster prototypes comes from the zero gradient condition

$$\frac{\partial J_{\text{hyb-g}}}{\partial v_i}=0 \quad \Rightarrow \quad -2\sum_{k=1}^{n}\xi_{ik}g_k(y_k-g_kv_i)=0,$$

which implies

$$\sum_{k=1}^{n}\xi_{ik}g_ky_k=v_i\sum_{k=1}^{n}\xi_{ik}g_k^2 \quad \Rightarrow \quad v_i=\frac{\sum_{k=1}^{n}\xi_{ik}g_ky_k}{\sum_{k=1}^{n}\xi_{ik}g_k^2}.$$

Finally, we need to partially differentiate the cost function with respect to g_k:

$$\frac{\partial J_{\text{hyb-g}}}{\partial g_k}=0 \quad \Rightarrow \quad -2\sum_{i=1}^{c}\xi_{ik}v_i(y_k-g_kv_i)=0,$$

which leads to

$$y_k\sum_{i=1}^{c}\xi_{ik}v_i=g_k\sum_{i=1}^{c}\xi_{ik}v_i^2 \quad \Rightarrow \quad g_k=y_k\frac{\sum_{i=1}^{c}\xi_{ik}v_i}{\sum_{i=1}^{c}\xi_{ik}v_i^2}.$$

References

[1] M.Y. Siyal, L. Yu, An intelligent modified fuzzy *c*-means based algorithm for bias field estimation and segmentation of brain MRI, Pattern Recognition Letters 26 (13) (2005) 2052–2062.

[2] L. Axel, J. Costanini, J. Listerud, Inhomogeneity correction in surface-coil MR imaging, American Journal of Roentgenology 148 (2) (1987) 418–420.

[3] A. Simmons, P.S. Tofts, G.J. Barker, S.R. Arrdige, Sources of intensity nonuniformity in spin echo images at 1.5T, Magnetic Resonance in Medicine 32 (1) (1994) 121–128.

[4] U. Vovk, F. Pernuš, B. Likar, A review of methods for correction of intensity inhomogeneity in MRI, IEEE Transactions on Medical Imaging 26 (3) (2007) 405–421.

[5] B.H. Brinkmann, A. Manduca, R.A. Robb, Optimized homomorphic unsharp masking for MR grayscale inhomogeneity correction, IEEE Transactions on Medical Imaging 17 (2) (1998) 161–171.

[6] B. Johnston, M.S. Atkins, B. Mackiewich, M. Anderson, Segmentation of multiple sclerosis lesions in intensity corrected multispectral MRI, IEEE Transactions on Medical Imaging 15 (2) (1996) 154–169.

[7] P. Vemuri, E.G. Kholmovski, D.L. Parker, B.E. Chapman, Coil sensitivity estimation for optimal SNR reconstruction and intensity inhomogeneity correction in phased array MR imaging, Lecture Notes in Computer Science (IPMI'05) 3565 (2005) 603–614.

[8] C.R. Meyer, P.H. Bland, J. Pipe, Retrospective correction of intensity inhomogeneities in MRI, IEEE Transactions on Medical Imaging 14 (1) (1995) 36–41.
[9] E.A. Vokurka, N.A. Watson, Y. Watson, N.A. Thacker, A. Jackson, Improved high resolution MR imaging for surface coils using automated intensity non-uniformity correction: feasibility study in the orbit, Journal of Magnetic Resonance Imaging 14 (5) (2001) 540–546.
[10] K. van Leemput, F. Maes, D. Vandermeulen, P. Suetens, Automated model-based bias field correction of MR images of the brain, IEEE Transactions on Medical Imaging 18 (10) (1999) 885–896.
[11] W.M. Wells III, W.E.L. Grimson, R. Kikinis, F.A. Jolesz, Adaptive segmentation of MRI data, IEEE Transactions on Medical Imaging 15 (4) (1996) 429–442.
[12] S. Ruan, B. Moretti, J. Fadili, D. Bloyet, Fuzzy Markovian segmentation in application of magnetic resonance images, Computer Vision and Image Understanding 85 (1) (2002) 54–69.
[13] Y. Zhang, M. Brady, S. Smith, Segmentation of brain MR images through a hidden Markov random field model and the expectation-maximization algorithm, IEEE Transactions on Medical Imaging 20 (1) (2001) 45–57.
[14] J.C. Bezdek, L.O. Hall, L.P. Clarke, Review of MR image segmentation techniques using pattern recognition, Medical Physics 20 (4) (1993) 1033–1048.
[15] D.L. Pham, J.L. Prince, Adaptive fuzzy segmentation of magnetic resonance images, IEEE Transactions on Medical Imaging 18 (9) (1999) 737–752.
[16] J. Derganc, B. Likar, F. Pernuš, Nonparametric segmentation of multispectral MR images incorporating spatial and intensity information, Progress in Biomedical Optics and Imaging 3 (1) (2002) 391–400.
[17] J.G. Sled, A.P. Zijdenbos, A.C. Evans, A nonparamtertic method for automatic correction of intensity nonuniformities, IEEE Transactions on Medical Imaging 17 (1) (1998) 87–97.
[18] B. Likar, A. Viergever, F. Pernuš, Retrospective correction of MR intensity inhomogeneity by information minimization, IEEE Transactions on Medical Imaging 20 (12) (2001) 1398–1410.
[19] J. Luo, Y. Zhu, P. Clarysse, I. Magnin, Correction of bias field in MR images using singularity function analysis, IEEE Transactions on Medical Imaging 24 (8) (2005) 1067–1085.
[20] C. Studholme, V. Cardenas, E. Song, F. Ezekiel, A. Maudsley, M. Weiner, Accurate template-based correction of brain MRI intensity distortion with application to dementia and aging, IEEE Transactions on Medical Imaging 23 (1) (2004) 99–110.
[21] D.W. Shattuck, S.R. Sandor-Leahy, K.A. Schaper, D.A. Rottenberg, R.M. Leahy, Magnetic resonance image tissue classification using a partial volume model, NeuroImage 13 (5) (2001) 856–876.
[22] M. Styner, C. Brechbuchler, G. Székely, G. Gerig, Parametric estimate of intensity inhomogeneities applied to MRI, IEEE Transactions on Medical Imaging 19 (3) (2000) 153–165.
[23] X. Li, L.H. Li, H.B. Lu, Z.G. Liang, Partial volume segmentation of brain magnetic resonace images based on maximum a posteriori probability, Medical Physics 32 (7) (2005) 2337–2345.
[24] A.W.C. Liew, Y. Hong, An adaptive spatial fuzzy clustering algorithm for 3-D MR image segmentation, IEEE Transactions on Medical Imaging 22 (9) (2003) 1063–1075.
[25] M.N. Ahmed, S.M. Yamany, N. Mohamed, A.A. Farag, T. Moriarty, A modified fuzzy *c*-means algorithm for bias field estimation and segmentation of MRI data, IEEE Transactions on Medical Imaging 21 (3) (2002) 193–199.
[26] H. Steinhaus, Sur la division des corp materiels en parties, in: Bulletin de l'Academie Polonaise des Science C1 III., IV, 1956, pp. 801–804.
[27] J.C. Bezdek, Pattern Recognition with Fuzzy Objective Function Algorithms, Plenum, New York, NY, 1981.
[28] R. Krishnapuram, J.M. Keller, A possibilistic approach to clustering, IEEE Transactions on Fuzzy Systems 1 (2) (1993) 98–110.
[29] M. Barni, V. Capellini, A. Mecocci, Comments on a possibilistic approach to clustering, IEEE Transactions on Fuzzy Systems 4 (3) (1996) 393–396.
[30] N.R. Pal, K. Pal, J.M. Keller, J.C. Bezdek, A possibilistic fuzzy *c*-means clustering algorithms, IEEE Transactions on Fuzzy Systems 13 (4) (2005) 517–530.
[31] J.L. Fan, W.Z. Zhen, W.X. Xie, Suppressed fuzzy *c*-means clustering algorithm, Pattern Recognition Letters 24 (9–10) (2003) 1607–1612.
[32] L. Szilágyi, S.M. Szilágyi, Z. Benyó, Analytical and numerical evaluation of the suppressed fuzzy *c*-means algorithm: a study on the competition in *c*-means clustering models, Soft Computing 14 (5) (2010) 495–505.
[33] R.N. Davé, Characterization and detection of noise in clustering, Pattern Recognition Letters 12 (11) (1991) 657–664.
[34] M. Menard, C. Damko, P. Loonis, The fuzzy c+2 means: solving the ambiguity rejection in clustering, Pattern Recognition 33 (7) (2000) 1219–1237.
[35] N.R. Pal, K. Pal, J.C. Bezdek, A mixed c-means clustering model, in: Proceedings of the 6th IEEE International Conference on Fuzzy Systems (FUZZ-IEEE), 1997, pp. 11–21.
[36] H. Timm, C. Borgelt, C. Döring, R. Kruse, An extension to possibilistic fuzzy cluster analysis, Fuzzy Sets and Systems 147 (1) (2004) 3–16.
[37] S.M. Szilágyi, L. Szilágyi, D. Iclănzan, L. Dávid, A. Frigy, Z. Benyó, Intensity inhomogeneity correction and segmentation of magnetic resonance images using a multi-stage fuzzy clustering approach, Neural Network World 19 (5) (2009) 513–528.
[38] L. Szilágyi, S.M. Szilágyi, Z. Benyó, Efficient feature extraction for fast segmentation of MR brain images, Lecture Notes in Computer Science (SCIA'07) 4522 (2007) 611–620.
[39] E. Anderson, The irises of the Gaspe peninsula, Bulletin of the American Iris Society 59 (1935) 2–5.
[40] A. Asuncion, D.J. Newman, UCI Machine Learning Repository. Irvine, CA: University of California, School of Information and Computer Science, 2007, Available at: http://www.ics.uci.edu/mlearn/MLRepository.html.
[41] L. Szilágyi, S.M. Szilágyi, Z. Benyó, in: Proceedings of the IEEE International Conference on Fuzzy Systems, A unified approach to c-means clustering models (2009) 456–461.
[42] Internet Brain Segmentation Repository, Available at: http://www.cma.mgh.harvard.edu/ibsr.